Journal of Applied Sciences

ISSN 1812-5654

science alert

ANSInet
an open access publisher
http://ansinet.com

Journal of Applied Sciences 12 (8): 736-744, 2012
ISSN 1812-5654 / DOI: 10.3923/jas.2012.736.744

Postural Balance of Humanoid Step Stance via Hybrid Space Formulation

[1]Zengshi Chen and [2]Weiwei Yong
[1]Lufkin Industries, Inc., 810 Oak Willow Drive, Missouri City, Texas, 77489, USA
[2]Guangdong Medical College, Zhanjiang, Guangdong, 524023, People's Republic of China

Abstract: This research studies the postural balance of a step stance through modeling, control, simulation and experimentation. The mathematical model of a five segment humanoid subject is developed. The redundant multi-variable system is projected onto a hybrid (Cartesian/joint) space with three degrees of freedom to make control easier. Based on the decoupled nonlinear system, a linear feedback control is designed to regulate the perturbation error. With the Lagrange method, a novel optimal bias control as a function of the system state, velocity and acceleration is designed to counteract the system main dynamics. The related balancing motion is performed by a human with markers on a force plate. The motion trajectories and the ground reaction forces are recorded. Comparison of the experimental and simulation results show that the proposed modeling and control strategy is capable of replicating the step stance balancing process. This research will promote understanding of mechanism of step stance postural balance for elder citizens and assist the relevant prosthesis design.

Key words: Step stance (SS), postural balance, fall, optimal bias, hybrid, ground reaction force

INTRODUCTION

Human posture has been a popular research area. Advanced filters have been used for human posture recognition (Tahir *et al*., 2007). A mechanism based on neural network is developed to classify human body postures (Tahir *et al*., 2006). The challenge to postural balance control is created when humans walk, run and stand. A human is an inherently unstable system unless a control action is continuously implemented (Winter, 1987). The capability of balance degenerates due to virtually all neuromusculoskeletal disorders (Byl, 1992). A pathology may not be obvious because the Central Nervous System (CNS) has ability to compensate for the loss of the function (Winter, 1995). The three major sensory systems are used in balance and posture control: The vision system, the "gyro" vestibular system and the somatosensory system (Horak *et al*., 1990). Due to the three separated sensory systems, a certain degree of redundancy can be used when one or two of the systems fails (Horak *et al*., 1990). Most of the work on balance have studied the function of each sensory system and the use of the redundancy if a system is dysfunctional (Diener *et al*., 1984).

The slow mobility of the elder at home is often involved in balance control (Committee Annual Report, 2004). Research on the fall of the elder covers many areas. Smart sensors are integrated to detect the falls of the elderly (Sixsmith and Johnson, 2004; Fu *et al*., 2008; Wu and Xue, 2008; Zigel *et al*., 2009; Doukas and Maglogiannis, 2011). Balance protheses are designed to prevent falls (Wall and Weinberg, 2003; Shi *et al*., 2009). Appropriate methods are developed to assess fall risk of the elder (Greene *et al*., 2010). However, using dynamics, control and simulation for fall research is scarce.

A human, modeled in the sagittal plane for a variety of research aims, can achieve a postural balance either in the Single Support Stance (SSS) (Kubica *et al*., 1995) or in the step stance (SS) (Rohlmann *et al*., 2001). Some human locomotion such as starting or termination of sitting (Rohlmann *et al*., 2001), getting onto or off the bed and termination of walking or running (Mu, 2004) ends up with balancing a SS posture. Lifting with a SS is a routine human manual task (Kollmitzer *et al*., 2002). In sports, a basketball player after a jump shot (Christgau, 1999) or a soccer kicker after heading a ball (Vogelsinger, 1970) or a skater gliding on a skate after propulsion of his leg (Allinger *et al*., 1997) often has to bring his state to a stable SS poise. Balancing SS postures for patients with locomotion disability is difficult (Patla *et al*., 1995). Ritual bow in SS was popular in the Chinese society (Chai and Chai, 1966). Study of those SS postural balances in locomotion, activity, sports and pathology can generate knowledge on improving performance, reducing injuries and facilitating gait rehabilitation.

The balance control of an open three-link human model in the SSS was reported (Koozekanani *et al*., 1983). The constrained motion of a five-link biped was studied

Corresponding Author: Zengshi Chen, Lufkin Industries, Inc., 810 Oak Willow Drive, Missouri City, Texas, 77489, USA

(Ceranowicz *et al*., 1980). The sway motion of a three-link biped in the SS was tested (Hemami and Wyman, 1979). In reality, SS motion satisfying a constraint always exists. In the SS, the biped can be modeled by the joint space orientation of its torso and the two Cartesian space variables that are the two hip translational positions. This strategy has been previously applied to a SS jump (Chen, 2006). It provides the minimal but sufficient number of the state variables to describe the SS movement of the biped.

The SS postural balance by modeling, simulation and experimentation is studied. The task is to bring the bipedal SS posture to a reference position without prescribing the entire trajectory except the target position and with the motion rigorously constrained to an invariant subspace (the space spanned by the motions of the subject for which the motion constraint is satisfied).

The model: A sagittal five link human subject in a step stance posture on flat ground is modeled. The subject has five segments: The two identical legs, the two identical thighs and a torso. The subject has the two ankle joints, the two knee joints and the two hip joints. Every joint is equipped with a purely rotational and frictionless actuator. The feet are assumed to be massless. Let m_i, G_i, I_i, X_i and θ_i be the mass, the gravity, the moment of inertia, the center of gravity and the orientation of the ith link, respectively. Let τ_i, F_{ih} and F_{iv} be the torque, the horizontal force and the vertical force acting on the ith joint, respectively. Let $\tau = (\tau_1\ \tau_2\ \tau_3\ \tau_4\ \tau_5\ \tau_6)^T$ where superscript T means "transpose". Let $\theta = (\theta_1\ \theta_2\ \theta_3\ \theta_4\ \theta_5)^T$. A schematic representation of the model is shown in Fig. 1a. The markers located on the subject for a SS stance posture balance experiment is shown in Fig. 1b. The detailed model is shown in Fig. 2. The detailed explanation of the parameters shown in Fig. 1 and 2 (Chen, 2006). In SS, the subject has three degrees of freedom. Once the subject controls them, the whole system is under control. Therefore, three state variables are enough to describe the system. The Cartesian and joint space formulation is effective. As shown by Chen (2006), this formulation consists of the hip position variables from the Cartesian space and the torso orientation from the joint space and the state equation is:

$$\dot{q} = \dot{q}$$
$$\ddot{q} = f(q, \dot{q}, \tau) \quad (1)$$

$$c_h = (k_1+l_1)\sin\theta_1+(k_2+l_2)\sin\theta_2-(k_4+l_4)\sin\theta_4(k_5+l_5\sin\theta_5 = L \quad (2)$$

$$C_V = (K_1+l_1)\cos\theta_1+(k_2+l_2)\cos\theta_2-(k_4+l_4)\cos\theta_4-(k_5+l_5)\cos\theta_5 = 0 \quad (3)$$

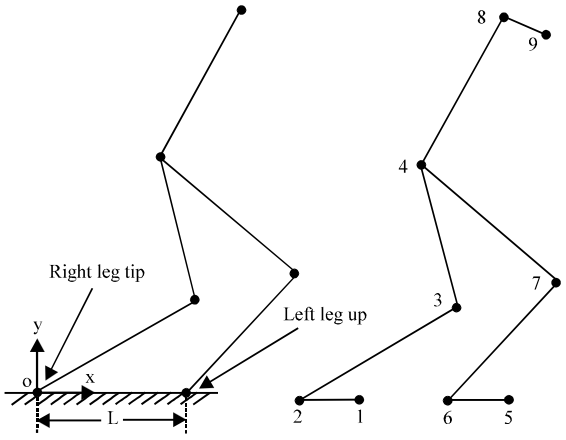

Fig. 1: (a) The kinematic model of a five-link human model, (b) The locations of the nine markers on the human subject

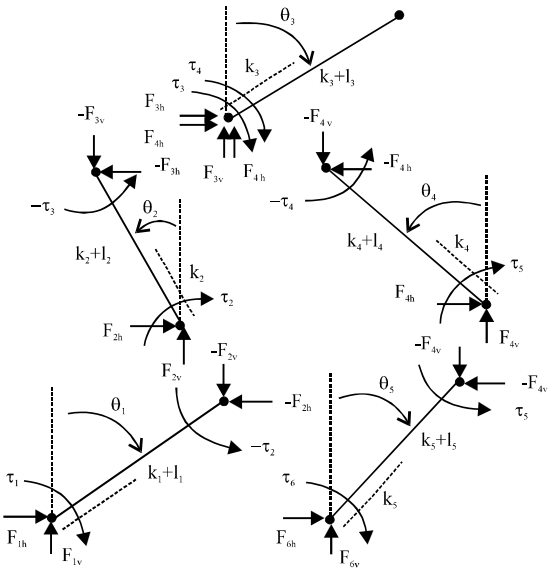

Fig. 2: The parameters of the biped when the segments are viewed separately

The controller: Equation 1 is linearized around an equilibrium point. A linear feedback is used to regulate the tracking error. An optimal nonlinear feed-forward control is used to cancel out the main dynamics. A step stance posture is balanced. The system trajectories, the ground reaction force and the conservation of the constraints are investigated.

Linear feedback controller: With the hip trajectory and the inverse kinematics, the joint angle profile for the SS (Chen, 2006). Let τ_s be the static bias torque when the subject is stationary with $q = q_s$, $\dot{q}_s = 0_{3\times1}$ and $\ddot{q}_s = 0_{3\times1}$

where $0_{3\times1}$ is a matrix of 3 rows and 1 column. When the subject is perturbed from its equilibrium, the state variables, their higher order derivatives and the torques are expressed in the two parts: the static part with the subscript s and the disturbed part with the subscript p as $q = q_s+q_p$, $\dot{q} = \dot{q}_p$ and $\ddot{q} = \ddot{q}_p$ where $\tau = \tau_s+\tau_p$ is the bias torque when the dynamics is considered. By Taylor expansion, the perturbation equation is written as:

$$\begin{bmatrix} \dot{q}_p \\ \ddot{q}_p \end{bmatrix} = \begin{bmatrix} 0_{3\times3} & I_{3\times3} \\ A_1 & A_2 \end{bmatrix} \begin{bmatrix} q_p \\ \dot{q}_p \end{bmatrix} + \begin{bmatrix} 0_{3\times6} \\ \bar{L} \end{bmatrix} \tau_P \tag{4}$$

Where:

$$A_1 = \frac{\partial f}{\partial q}|_{q_s,\dot{q}_s,\tau_s}, A_2 = \frac{\partial f}{\partial \dot{q}}|_{q_s,\dot{q}_s,\tau_s} = 0_{3\times3}$$

and:

$$\bar{L} = \frac{\partial f}{\partial \tau}|_{q_s,\dot{q}_s,\tau_s}$$

$I_{3\times3}$ is a 3×3 identity matrix. $0_{3\times3}$ and $0_{3\times6}$ are the 3×3 and 3×6 zero matrices, respectively. The desired state equation of the decoupled system is:

$$\begin{bmatrix} \dot{q}_p \\ \ddot{q}_p \end{bmatrix} = \begin{bmatrix} 0_{3\times3} & I_{3e} \\ K_1 & K_2 \end{bmatrix} \begin{bmatrix} q_p \\ \dot{q}_p \end{bmatrix} \tag{5}$$

where:

$$K_1 = \begin{bmatrix} -\eta_1 * \eta_2 & 0 & 0 \\ 0 & -r_{21} * r_{22} & 0 \\ 0 & 0 & -r_{31} * r_{32} \end{bmatrix}$$

and:

$$K_2 = \begin{bmatrix} \eta_1 + \eta_2 & 0 & 0 \\ 0 & r_{21} + r_{22} & 0 \\ 0 & 0 & r_{31} + r_{32} \end{bmatrix}$$

One can select the appropriate eigenvalues r_{i1}, and r_{i2} with i = 1 to 3 to obtain the desired system response. The linear control of $\tau_p = K_p(q-q_s)+K_v(\dot{q}-\dot{q})$is selected where K_p and K_v are the position and velocity gain matrices of 6×3, respectively. Comparing Eq. 4 and 5, one has the desired gain matrices in terms of:

$$K_p = \bar{L}^T\left(\bar{L}\bar{L}^T\right)^{-1}(K_1 - A_1) \tag{6}$$

$$K_V = \bar{L}^T\left(\bar{L}\bar{L}^T\right)^{-1}(K_2 - A_2) \tag{7}$$

Optimal bias control: When the subject is stationary, $\dot{q}_s = 0$ and $\ddot{q}_s = 0$. However, dynamics exists before a subject converges to a stable SS posture. Therefore, unlike the conventional bias method, the velocity and acceleration in the bias torque compensation is taken into account. Defining the dynamic bias torque with the denotation of τ_d. Since there are more joint torques than the segments of the subject, τ_d is not unique. However, a unique solution exists to minimize a criterion function such as:

$$0.5\tau_d^T\tau_d$$

The dynamic rotational equations of the subject are:

$$\begin{aligned} I_1\ddot{\theta}_1 &= A_{11}F_1 + A_{12}F_2 + A_{13}\tau_d\, 0.5\tau_d^T\tau_d \\ I_2\ddot{\theta}_2 &= A_{21}F_2 + A_{22}F_3 + A_{23}\tau_d \\ I_3\ddot{\theta}_3 &= A_{31}F_3 + A_{32}F_4 + A_{33}\tau_d \\ I_4\ddot{\theta}_4 &= A_{41}F_4 + A_{42}F_5 + A_{43}\tau_d \\ I_5\ddot{\theta}_5 &= A_5F_5 + A_{52}F_6 + A_{53}\tau_d \end{aligned} \tag{8}$$

where, A_{ij} for i or j = 1 to 3 is defined by Chen (2006). The dynamic translational equations of the subject are:

$$\begin{aligned} M_1\ddot{X}_1 &= G_1 + F_1 - F_2 \\ M_2\ddot{X}_2 &= G_2 + F_2 - F_3 \\ M_3\ddot{X}_3 &= G_3 + F_3 + F_4 \\ M_4\ddot{X}_4 &= G_4 + F_5 - F_4 \\ M_5\ddot{X}_5 &= G_5 + F_6 - F_5 \end{aligned} \tag{9}$$

$\ddot{X}_i$ is the function of Θ and $\ddot{\Theta}$. Solving Eq. 9 for F_2, F_3, F_4, F_5 and F_6 in terms of F_1 renders:

$$D_1F_1+D_2 = D\tau_d \tag{10}$$

where, D_1, D_2 and D are defined by Chen (2006). Assuming F_1 is an arbitrary constant vector and $D_1F_1+D_2 = D_3$ one can minimize the criterion function of:

$$0.5\tau_d^T\tau_d$$

with the constraint equation of $D\tau_d-D_3 = 0_{5\times1}$. Let the Lagrange equation be:

$$L = 0.5\tau_d^T\tau_d + \lambda^T(D\tau_d - D_2)$$

where, λ is a vector of five Lagrange multipliers corresponding to the five constraint equations. Then, the equilibrium point of the subject from the local minimization could be found as:

$$(\frac{\partial \bar{L}}{\partial \tau_d})^T = \tau_d + D^T\lambda = 0_{6\times1} \quad (11)$$

$$(\frac{\partial \bar{L}}{\partial \tau_d})^T = D\tau_d - D_3 = 0_{5\times1} \quad (12)$$

Multiplying Eq. 10 by D and solving it for λ enders:

$$\lambda = -(DD^T)^{-1}D_3 \quad (13)$$

Substituting Eq. 13 into Eq. 11 renders:

$$\tau_d = D^T(DD^T)^{-1}(D_1F_1+D_2) \quad (14)$$

Now:

$$0.5\tau_d^T\tau_d$$

is an explicit function of F_1 and it can be minimized with respect to F_1. The criterion function becomes:

$$0.5\tau_d^T\tau_d = 0.5F_1^TD_1^T(DD^T)^{-1}D_1F_1 + F_1^TD_1^T(DD^T)^{-1}D_2 + 0.5D_2^T(DD^T)^{-1}D_2 \quad (15)$$

With the symmetrical property of $D^T_1(DD^T)^{-1}D_1$, F_1 is found from the partial differentiation of:

$$0.5\tau_d^T\tau_d$$

with respect to F_1. One has:

$$F_1 = -(D_1^T(DD^T)^{-1}D_1)^{-1}D_1^T(DD^T)^{-1}D_2 \quad (16)$$

Equation 14 becomes:

$$\tau_d = D^T(DD^T)^{-1}(-D_1(D_1^T(DD^T)^{-1}D_1)^{-1}D_1^T(DD^T)^{-1}D_{21} + D_2) \quad (17)$$

τ_d will be used as τ_s.

RESULTS

Simulation parameters: The horizontal distance of the two feet is taken as 0.2655 cm. The values of the parameters are shown in Table 1. The equilibrium point of the subject is taken as $q_s = [0.1328\ (m)\ 1.0431\ (m)\ 0\ (rad)]^T$, $\dot{q}_s = (0\ 0\ 0)^T$ and $\ddot{q}_s = (0\ 0\ 0)^T$. The related dynamic bias torque in the unit of N*m is τ_s = (-9.67 21.73 -1.2 1.2 1.63 -6.64). The poles of each decoupled system are selected as $r_{i1} = r_{i2}$. This results in:

Table 1: Parameters of the subject

Segment No.	m_i (kg)	I_i (kg m^2)	k_i (m)	l_i (m)
1	4	0.065	0.3	0.23
2	8	0.126	0.3	0.23
3	55	3.4	0.35	0.37
4	8	0.126	0.3	0.23
5	4	0.065	0.3	0.23

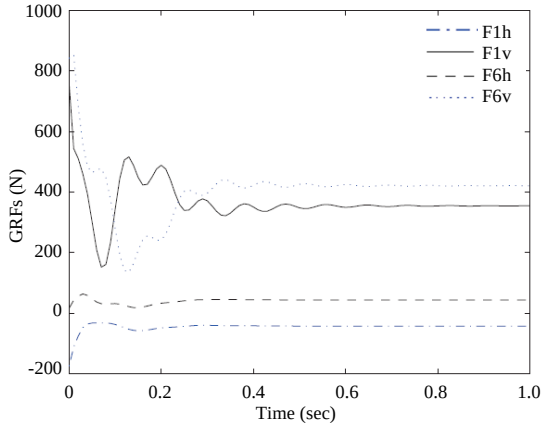

Fig. 3: The four ground reaction forces in the step stance postural balance

$$A_1 = 0_{3\times3}$$

$$\bar{L} = \begin{bmatrix} -0.0405 & 0.1489 & -0.1780 & -0.1101 & 0.0106 & 0.0299 \\ -0.05 & 0.1085 & -0.0687 & -0.0602 & 0.0882 & -0.0382 \\ 0.077 & -0.2828 & 0.4367 & 0.3078 & -0.0202 & -0.0568 \end{bmatrix}$$

$$K_p = \begin{bmatrix} 678.62 & 453.81 & 341.27 \\ -4445.8 & -164.69 & -1749.3 \\ -621.34 & -371.46 & -607.07 \\ -3709.9 & 371.46 & -1673.9 \\ 1774.6 & -1621.6 & 406.02 \\ -2453.2 & 1167.8 & -747.29 \end{bmatrix},$$

$$K_v = \begin{bmatrix} 90.48 & 60.51 & 45.50 \\ -592.78 & -21.96 & -233.24 \\ -82.84 & -49.53 & -80.94 \\ 494.66 & 49.53 & -223.18 \\ 236.61 & -216.22 & 54.14 \\ -327.10 & 155.71 & -99.64 \end{bmatrix}$$

Simulation results: Figure 3 shows that the ground reactions forces (GRFs) converge to their equilibrium points. In the entire response, $F_{1h} \leq 0$, $F_{6h} \geq 0$, $F_{1v} \geq 0$ and $F_{6v} \geq 0$. Figure 4 shows that the position variables converge to their static values. The Cartesian space variables h_x and h_y, are monotonically increasing. The joint space variable, θ_3, after experiencing a slight overshoot, converges. The hip is moving forward and upward. The torso rotates clockwise first and then counterclockwise to the vertical stance. Figure 5 shows the trajectories of the six joint torques. Their magnitudes can be generated by human beings and are hence

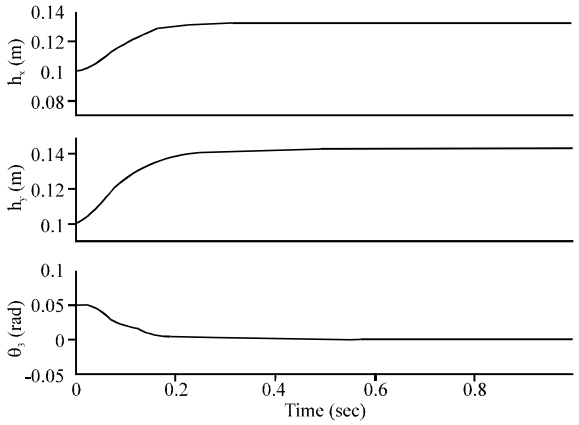

Fig. 4: The simulated trajectories of the state variables: h_x, h_y and θ_3 in the Cartesian and joint space

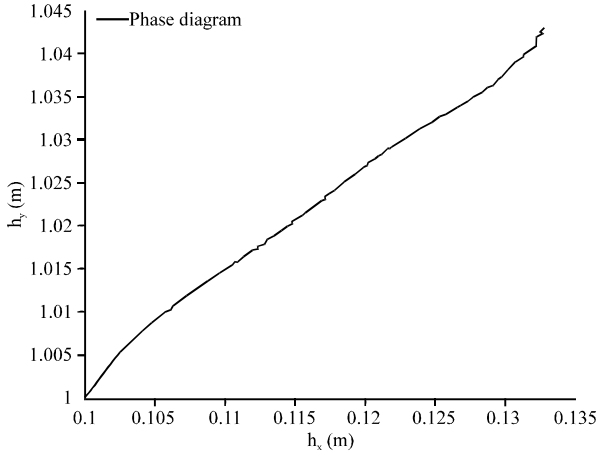

Fig. 5: The simulated trajectories of the state variables: h_x, h_y and θ_3 in the Cartesian and joint space

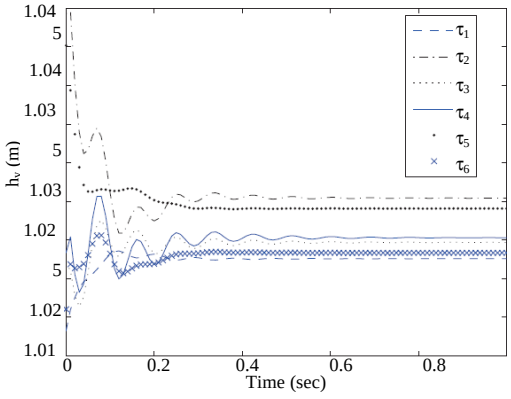

Fig. 6: The trajectories of the joint torques: τ_1, τ_2, τ_3, τ_4, τ_5 and τ_6

reasonable. Figure 6 shows the hip trajectory of the subject in the sagittal plane. Apparently, the hip is

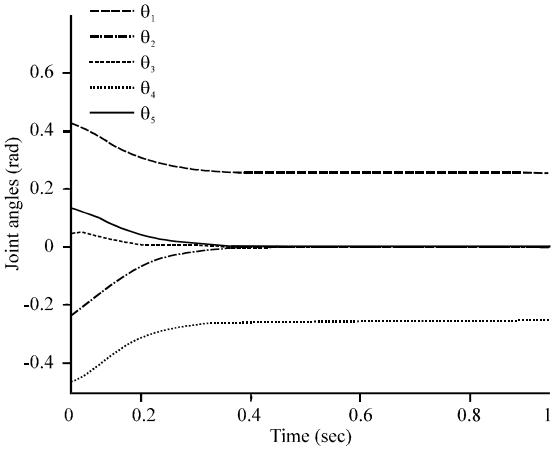

Fig. 7: The simulated trajectories of the joint angles in the joint space: θ_1, θ_2, θ_3, θ_4, θ_5 and θ_6

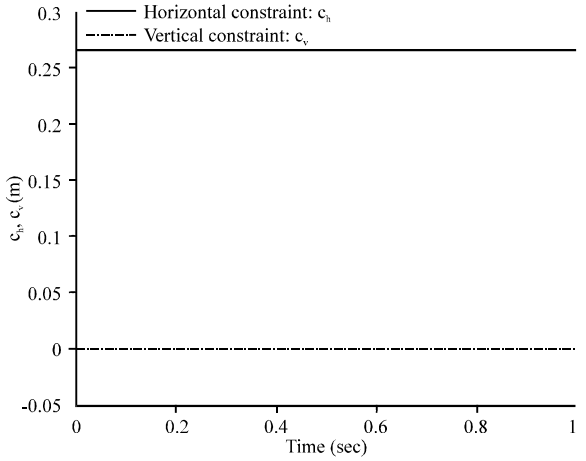

Fig. 8: The constrained horizontal and vertical distances of the feet of the subject

moving in a nonlinear curve. Figure 7 shows the convergence of the five angular state variables in the joint space to their equilibrium values. Figure 8 shows that the physical constraints between the feet are maintained in the entire response. Figure 9 shows the sequential stick diagrams of the subject that is being brought to the equilibrium point from the initial condition.

Experimental results: In this experiment, the step stance postural balance is performed by a subject who lands in SS (the two feet touch the ground simultaneously) on the force plates and stabilizes her post-impact posture. An Optotrak 3020 system and two Bertec force platforms were used to collect the kinematic and GRF data from a young, healthy female subject. The two tracking markers

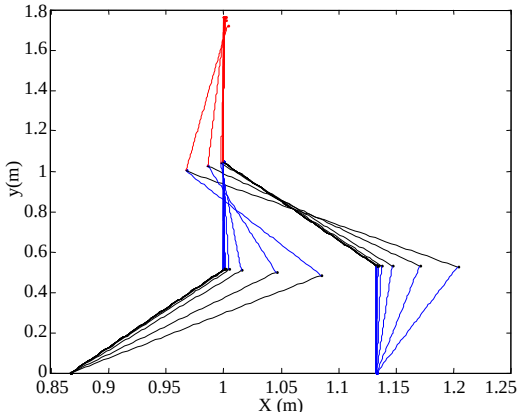

Fig. 9: The stick diagram of the subject in the step stance postural balance

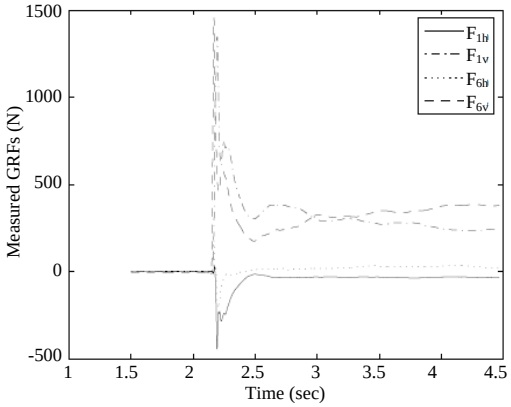

Fig. 10: Measured ground reaction forces in a step stance after a landing.

(infrared light-emitting diodes) were attached to the skin over specific boney landmarks on the hip and the shoulder. The marker locations are shown in Fig. 1b. As the subject moved, the Optotrak system tracked the marker positions and simultaneously calculated precise three-dimensional data for each. The sampling frequency was 100 Hz for the motion data and 1000 Hz for the GRFs. The data was filtered by a low pass Butterworth filter with the cutoff frequency of 6 Hz for motion and 15 Hz for GRFs. Each link of the subject is approximated as a rigid body. Assuming the coordinates of the markers on the hip as (h_x, h_y) and on the shoulder as (s_x, s_y), one computes the rotational angle of the torso as:

$$\theta_3 = \text{atan2}(s_y-h_y, s_x-h_x) \quad (18)$$

The subject is instructed to land on the force platforms in SS and bring her posture to a reference position from the post-impact stance. Six experiments were done. After each impact, a natural postural balance motion is executed by the subject. It is noticed that the balance motions performed by the subject are similar to the motion in the simulation. That is, with the initial velocity, the subject moves her hip upward and forward while rotating her torso counterclockwise. The subject does not have any slippage during postural stabilization. Figure 10 demonstrates the recorded ground reaction forces. Ignoring impact impulses, one notices that the measured ground reaction forces take the similar overall pattern as the simulated ones. After landing, almost instantaneously, F_{h1} and F_{h6} fall to their minima and F_{v1} and F_{v6} increase to their maxima. Then, both F_{h1} and F_{h6} increase. F_{h1} stays below zero and converges to a negative value. F_{h6} crosses zero to converge to a positive constant. After the subject

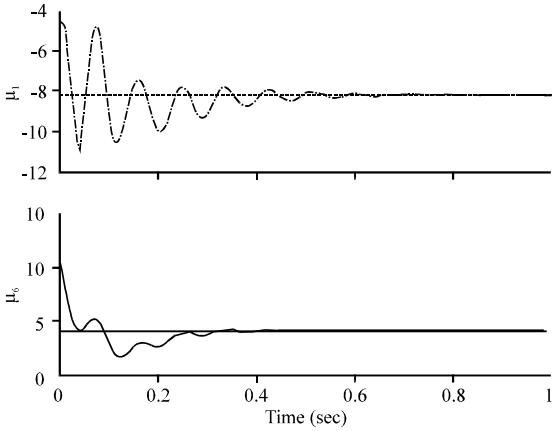

Fig. 11: The top panel shows the friction coefficient μ_1 and its average value. The actual coefficient is $|\mu_1|$. The bottom panel shows the friction coefficient μ_6 and its average value

is brought to standstill, the GRFs converge to constants with F_{h1} 30 N, F_{h6} 35 N, F_{v1} 270 N and F_{v6} 350 N. Both F_{h1} and F_{h6} are less than or equal to 0 in the beginning of the landing because the inertial momentum of the subject tends to throw her forward. F_{h1} and F_{h6} provide the counter-momentum to decelerate the subject to rest in the horizontal direction. During the standstill time, the subject shifts her body weight from her right lower limb to her left lower limb.

In the simulation, since the initial perturbation is comparatively small with a slight throwing-forward momentum, thereafter, F_{h6} can start from a value close to zero and F_{h1} starts from a negative value. The phenomenon of shifting the body weight by the simulated subject is also observed in the simulation. In the

beginning, the majority of the weight is supported by the left lower limb such as $F_{v6} = F_{v1}$. In the sequential short interval, the weight is shifted to the right lower limb such as $F_{v1} = F_{v6}$. Finally, the weight is shifted back to the left lower limb such as $F_{v6} = F_{v1}$. The coincidence of the results from the simulation and experiment provides the conviction that the CNS of humans may be able to choose the minimal number of variables, adopt a simple control and stabilize human SS postures. In Fig. 11, the top panel shows μ_1, the friction coefficient of the right foot with the force plate over the time and its average value; the bottom panel shows μ_6, the friction coefficient of the left foot with the force plate over the time and its average value. Inspecting Fig. 11, one concludes that the friction coefficients required in the simulation can be provided by the force plates because the measured forces show that the force plates can provide the much larger friction coefficients.

DISCUSSION

Most of the existing postural balance research is confined to the following categories: (1) kinematics and measurement, (2) statics, (3) dynamics with the simplified model (4) dynamics with the simplified control. As for (1), an example is the study for the changes in postural sway and strategy elicited by lumbar extensor muscle fatigue (Madigan *et al*., 2006). Whole-body movement and ground reaction force data of twelve healthy male participants were recorded and used to calculate mean body posture and variability of center of mass, center of pressure and joint kinematics during quiet standing. As for (2), an example is the study of the impact of a human with the environment (Zheng and Hemami, 1984). The contact of the two feet in parallel with the ground is studied. The transient dynamics in the postural balance is ignored in the integration. As for (3), an example is the study of sway motion through a damper or spring model (Dijkstra, 2000). The damper and spring are connected to a stick representing the human body that itself is over-simplified. As for (4), an example is the computer simulation of postural balance through a recursive approach and linearization (Koozekanani et al., 1983). The human is modeled as a multi-link rigid body system with one contact point on the ground. Only linear control is used for postural balancing.

The proposed method in this paper overcomes the drawbacks of the above approaches. It models, controls and simulates a human SS postural balance. The dynamics model takes into account many physical details of an actual human. The optimal control is based on the rigorous analysis and derivation. The under-actuation of the system in the joint space is avoided by modeling the system in the Cartesian and joint space. With the inverse kinematics mapping from the Cartesian space to the joint space, the system during SS postural balance is constrained to an invariant subspace in which the state of the biped starts, roams and converges. Simulations give one the flexibility to study a hypothetical situation, such as bringing a SS posture from one to another. In particular, when the similar postural balance is executed by a real subject, the GRFs from the measurement and the GRFs from the simulation basically comply with each other. Although the subject in the experiment does not exactly bring her posture to the equilibrium set up in the simulation, the values of the converged GRFs in the experiment are still close to the optimal solution. One may infer that humans have a tendency to minimize their energy expenditure when stabilizing and maintaining their postures. The proposed method faithfully reproduces the SS postural balance which is common in sport competition and humanoid daily balance control. The responses of the ground reaction forces tell that the gravity of the body shifts between the lower limbs frequently and easily. Only if an elder is physically still strong or carries a prosthesis may he avoid a fall during those subconscious shifts of the body weight. In SS balance, for the Cartesian and joint space model, the hip cannot be perturbed too far from the equipoise. Otherwise, the inverse kinematics will have no solution. This may hint that an elder should refrain from strong motions in order to avoid a fall. The low friction of the certain floors and the weak vertical ground reactions an elder provides may cause him to slip and stumble.

The proposed method has a few disadvantages which should be addressed in the future study. The model under study is confined to the sagittal plane although sometimes a posture is balanced in the three-dimensional space. The proposed model is still simple since neither the feet nor the arms are considered. The joint torques instead of the muscle forces are used in the model. Although the optimal bias control is used, the central nerve system control that is closest to the nature is not studied. An actual fall motion has not been simulated.

REFERENCES

Allinger, T.L. and A.J. van den Bogert, 1997. Skating technique for the straights, based on the optimization of a simulation model. Med. Sci. Sports Exerc., 29: 279-286.

Byl, N.N., 1992. Spatial orientation to gravity and implications for balance training. Orthop. Phys. Ther. Clin. North Am., 1: 207-242.

Ceranowicz, A., B. Wyman and H. Hemami, 1980. Control of constrained systems of controllability index two. IEEE Trans. Automatic Control, 25: 1102-1111.

Chai, C. and W. Chai, 1966. Book of Rites. Lyle Stuart, New York, ISBN: 978-0821601075.

Chen, Z., 2006. Dynamics and Control of Collision of Multi-Link Humanoid Robots with a Rigid or Elastic Object. The Ohio State University, Columbs, Ohio, ISBN: 9780542823350, Pages: 207.

Christgau, J., 1999. The Origins of the Jump Shot: Eight Men who Shook the World of Basketball. University of Nebraska Press, USA, ISBN: 9780803263949, Pages: 220.

Committee Annual Report, 2004. Sacramento county elder death review team: Annual report, committee report. Broadway, Sacramento, California. http://www.edrtsac.org/2004%20EDRT%20Report%20Final%20.pdf

Diener, H.C., J. Dichgans, M. Bacher and B. Gompf, 1984. Quantification of postural sway in normals and patients with cerebellar diseases. Electroencephalogr. Clin. Neurophysiol., 57: 134-142.

Dijkstra, T.M.H.,. 2000. A gentle introduction to the dynamic set-point model of human postural control during perturbed stance.. Human Movement Sci., pp: 567 -595.

Doukas, C.N. and I. Maglogiannis, 2011. Emergency fall incidents detection in assisted living environments utilizing motion, sound and visual perceptual components. IEEE Trans. Inform. Technol. Biomed., 15: 277-289.

Fu, Z., T. Delbruck, P. Lichtsteiner and E. Culurciello, 2008. An address-event fall detector for assisted living applications. IEEE Trans. Biomed. Circuits Syst., 2: 88-96.

Greene, B.R., A. O`Donovan, R. Romero-Ortuno, L. Cogan, C.N. Scanaill and R.A. Kenny, 2010. Quantitative falls risk assessment using the timed up and go test. IEEE Trans. Biomed. Eng., 57: 2918-2926.

Hemami, H. and B. Wyman, 1979. Modeling and control of constrained dynamic systems with application to biped locomotion in the frontal plane. IEEE Trans. Automatic Control, 24: 526-535.

Horak, F.B., L.M. Nashner and H.C. Diener, 1990. Postural strategies associated with somatosensory and vestibular loss. Exp. Brain Res., 82: 167-177.

Kollmitzer, J., L. Oddsson, G.R. Ebenbichler, J.E. Giphart and C.J. DeLuca, 2002. Postural control during lifting. J. Biomech., 35: 585-594.

Koozekanani, S.H., K. Barin, R.B. McGhee and H.T. Chang, 1983. A recursive free-body approach to computer simulation of human postural dynamics. IEEE Trans. Biomed. Eng., 30: 787-792.

Kubica, E.G., D. Wang and D.A. Winter, 1995. Modelling balance and posture control mechanisms of the upper body using conventional and fuzzy techniques. Gait Posture, 311: 111-111.

Madigan, M.L., B.S. Davidson and M.A. Nussbaum,. 2006. Postural sway and joint kinematics during quiet standing are affected by lumbar extensor fatigue.. Human Movement Sci., pp: 788 -799.

Mu, X.P., 2004. Dynamics and motion regulation of a five link biped robot walking in the sagittal plane. Ph.D. Thesis, The University of Manitoba, Canada.

Patla, A.E., J.S. Frank, D.A. Winter, E. Roy, C. Silcher and A. Adkin, 1995. Effects of age and parkinsons disease on strategies for avoiding above ground obstacles during locomotion. Gait Posture, 3: 104-104.

Rohlmann, A., U. Arntz, F. Graichen and G. Bergmann, 2001. Loads on an internal spinal fixation device during sitting. J. Biomech., 34: 989-993.

Shi, G., C.S. Chan, W.J. Li, K.S. Leung, Y. Zou and Y. Jin, 2009. Mobile human airbag system for fall protection using MEMS sensors and embedded SVM classifier. IEEE Sensors J., 9: 495-503.

Sixsmith, A. and N. Johnson, 2004. A smart sensor to detect the falls of the elderly. IEEE Pervasive Comput., 3: 42-47.

Tahir, N.M., A. Hussain, S.A. Samad, H. Husain and M.M. Mustafa, 2006. Eigenposture for classification. J. Applied Sci., 6: 419-424.

Tahir, N.M., A. Hussain, S.A. Samad, H. Husain and A.T.B. Jin, 2007. On the use of advanced correlation filters for human posture recognition. J. Applied Sci., 7: 2947-2956.

Vogelsinger, H., 1970. Winning Soccer Skills and Techniques. Parker Publishing Company, Englewood Cliffs, New Jersey, Pages: 282.

Wall, C. and M.S. Weinberg, 2003. Balance prostheses for postural control. IEEE Eng. Med. Biol. Mag., 22: 84-90.

Winter, D.A., 1987. Sagittal plane balance and posture in human walking. IEEE Eng. Med. Biol. Mag., 6: 8-11.

Winter, D.A., 1995. Human balance and posture control during standing and walking. Gait Posture, 3: 193-214.

Wu, G. and S. Xue, 2008. Portable pre-impact fall detector with inertial sensors. IEEE Trans. Neural Syst. Rehabil. Eng., 16: 178-183.

Zheng, Y.F. and H. Hemami,. 1984. Impact effects of biped contact with the environment.. IEEE Trans. Syst Man Cybern., .,437 -443.

Zigel, Y., D. Litvak and I. Gannot, 2009. A method for automatic fall detection of elderly people using floor vibrations and sound-Proof of concept on human mimicking doll falls. IEEE Trans. Biomed. Eng., 56: 2858-2867.